ACS APPLIED MATERIALS & INTERFACES

Research Article

www.acsami.org

Long-Term Air-Stable *n*-Channel Organic Thin-Film Transistors Using 2,5-Difluoro-1,4-phenylene-bis{2-[4-(trifluoromethyl)phenyl]acrylonitrile}

Shuichi Nagamatsu,*[,†] Shinya Oku,[‡,⊥] Kouji Kuramoto,[§] Tetsuji Moriguchi,[§] Wataru Takashima,[∥] Tatsuo Okauchi,[§] and Shuzi Hayase[‡]

[†]Department of Computer Science and Electronics, Kyushu Institute of Technology, 680-4 Kawazu, Iizuka, Fukuoka 820-8502, Japan

[‡]Graduate School of Life Science and System Engineering, Kyushu Institute of Technology, 2-4 Hibikino, Wakamatsu-ku, Kitakyushu, Fukuoka 808-0196, Japan

[§]Department of Material Science, Kyushu Institute of Technology, 1-1 Sensuicho, Tobata-ku, Kitakyushu, Fukuoka 804-8550, Japan

[∥]Research Center for Advanced Eco-Fitting Technology, Kyushu Institute of Technology, 2-4 Hibikino, Wakamatsu-ku, Kitakyushu, Fukuoka 808-0196, Japan

Supporting Information

ABSTRACT: A long-term air-stable *n*-type organic semiconductor, 2,5-difluoro-1,4-phenylene-bis{2-[4-(trifluoromethyl)phenyl]acrylonitrile}, was synthesized by a high-yield simple procedure of Knoevenagel condensation with aldehyde and acetonitrile derivatives. A fabricated organic thin-film transistor (OTFT) using this compound exhibited good *n*-channel OTFT properties with a high electron mobility of 0.17 $cm^2 V^{-1} s^{-1}$ and an on/off current ratio of 10^6 under both vacuum and ambient air operation. After storage in ambient air for 1 year, a stored *n*-channel OTFT still shows good *n*-channel OTFT performance with little degradation in ambient air operation.

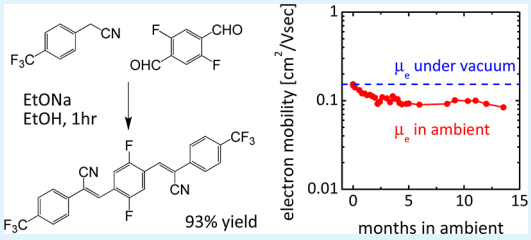

KEYWORDS: *n-type organic semiconductor, Knoevenagel condensation, long-term air stability, high electron mobility, organic thin-film transistors, organic inverter*

1. INTRODUCTION

Organic semiconductors have attracted much attention because they offer low-cost, flexible, and throwaway plastic electronics, such as organic solar cells, flexible display, or radiofrequency identification (RFID) tags. Because an organic thin-film transistor (OTFT) is the most fundamental electronic device in plastic electronics, improvements of their performance are strongly desired.[1−3] The development of a new organic semiconductor is the most important approach for providing intrinsic and potentially high-performance plastic electronic devices. For an organic inverter that is a basic logic device of integrated logic circuits, the complementary structure with both *p*- and *n*-channel OTFTs is required in logic devices with high-impedance and low-power consumption.[4] However, *n*-channel OTFT characteristics easily vanished after exposure to ambient air. The air stability of *n*-type organic semiconductors is necessary for the stable operation of organic logic circuits in ambient air.

Providing *n*-type organic semiconductors that exhibit air stability is strongly desired in this field. Recently, a variety of air-stable *n*-type organic semiconductors, including small organics and polymers, have been proposed.[5−20] Two main factors, a deep energy level of the lowest unoccupied molecular orbital (LUMO) and dense molecular packing with large van der Waals radius atom moieties, were possibly preventing the degradation of *n*-type transport characteristics in ambient air. The deep LUMO level below −4.1 eV prevents the redox reactions with atmospheric oxidants as chemical barriers, and the dense molecular packing protects the diffusion of atmospheric oxidants into π-conjugated core units of organic semiconductors as physical barriers.[8,9] On the other hand, the synthetic difficulty has probably precluded the identification of a candidate for wide use as an air-stable *n*-type organic semiconductor. For the further spread of the plastic electronics, simple procedures for the synthesis of air-stable *n*-type organic semiconductors are also strongly desired for industrial applications.

We previously reported an air-stable *n*-channel OTFT using 1,4-phenylene-bis{2-[4-(trifluoromethyl)phenyl]acrylonitrile} (compound **1** in Scheme 1), synthesized from commercially available terephthalaldehyde and 4-(trifluoromethyl)-phenylacetonitrile by a simple high-yield procedure of Knoevenagel condensation.[21] Compound **1** has an electron-withdrawing group (EWG)-substituted structure of distyr-

Received: October 17, 2013
Accepted: January 23, 2014
Published: March 12, 2014

Scheme 1. Chemical Structure of Compounds 1 and 2

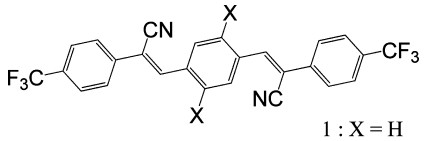

ylbenzene, which is one of the air-stable *p*-type organic semiconductors,[12,22] and is an oligomer of cyano-substituted poly(*p*-phenylenevinylene), which is one of the *n*-type light-emitting polymers.[23,24] Compound **1** has a deep LUMO energy level (E^{LUMO}) of −4.1 eV calculated with a highest occupied molecular orbital (HOMO) energy level (E^{HOMO}) estimated by photoelectron yield spectroscopy (PYS) and an energy band gap (E_g) of 2.6 eV estimated by the optical absorption spectra edge. An OTFT using compound **1** showed a high electron mobility (μ_e) of 0.127 $cm^2\ V^{-1}\ s^{-1}$ from a saturated regime under vacuum operation and good air resistivity of μ_e degradation of 4% as the percentage decrease in mobility ($\Delta\mu$) under vacuum operation after storage in ambient air for 1 month. However, this OTFT in ambient operation showed a $\Delta\mu$ of 76% degraded electron mobility after storage in ambient air for 1 day. The air stability of compound **1** is insufficient for stable operation of an organic logic circuit.

Here we report the improved air stability of the *n*-channel OTFT using a newly synthesized similarly structured compound having fluorine atom substitution, 2,5-difluoro-1,4-phenylene-bis{2-[4-(trifluoromethyl)phenyl]acrylonitrile} (compound **2**). Compound **2** was synthesized successfully by simple Knoevenagel condensation with a high yield of 93% (Scheme 2). After substitution with further EWG moieties, or a fluorine atom, compound **2** has a LUMO energy level deeper than that of compound **1**. The OTFT using compound **2** shows good *n*-channel OTFT properties and extremely long-term air stability that can be attributed to the deep LUMO energy level.

2. EXPERIMENTAL SECTION

2.1. Instrument. ^1H nuclear magnetic resonance (NMR) spectra were recorded on a Bruker Avance 400 spectrometer (400 MHz) in $CDCl_3$. ^{13}C and ^{19}F NMR spectra were recorded on a JEOL JNM-A500 spectrometer (500 MHz) in $CDCl_3$ or THF-d_8. Chemical shifts are reported as parts per million relative to an internal TMS standard (^1H and ^{13}C) and and an internal C_6F_6 standard (δ −164.9). Gas chromatography−mass spectrometry data were obtained using a JEOL JMS-SX102A instrument. Cyclic voltammetry (CV) measurements of the compounds were performed in a dichloromethane solution with 0.1 M tetrabutylammonium hexafluorophosphate ($TBAPF_6$) as the supporting electrolyte, a Pt disk as the working electrode, a Pt wire as the counter electrode, and a Ag/Ag^+ wire as the reference electrode using a HOKUTO HZ-5000 instrument at a scan rate of 50 mV/s. The surface morphology of the deposited film of compound **2** was investigated by atomic force microscopy (AFM) analysis performed using a JEOL JSPM-5200 instrument. The molecular orientation in the deposited film of compound **2** was investigated by synchrotron-sourced grazing incident X-ray diffraction (GIXD) analyses performed on beamline BL46XU of SPring-8 (JASRI) equipped with an ATX-GSOR instrument (Rigaku). For AFM and GIXD analysis, compound **2** was deposited by thermal evaporation on a silicon wafer with naturally grown silicon dioxide.

2.2. Materials. Commercially available chemicals were used without further purification. All reactions were conducted under an atmosphere of dry nitrogen. 2,5-Difluoroterephthalaldehyde (**4**) was prepared from 2,5-difluoro-1,4-dibromobenzene. Compound **2** was synthesized by Knoevenagel condensation of the 2,5-difluoroterephthalaldehyde (**4**) with 4-(trifluoromethyl)phenylacetonitrile.

2.3. Device Fabrication and Characterization. Bottom-gate top-contact-type OTFTs were constructed on highly doped *n*-type silicon wafers covered with 300 nm thick silicon dioxide, providing a capacitance per unit area (C_{ins}) of 10 nF cm^{-2}. Compound **2** was deposited on a bare silicon dioxide surface by a thermal evaporation method without controlling the substrate temperature; 40 nm thick gold source-drain electrodes were evaporated on top of the organic semiconductor films though a shadow mask, defined by a channel length (L) of 20 μm and a channel width (W) of 2 mm. OTFT characteristics were measured with a computer-controlled source-measure unit (Keithley2612) and were determined under vacuum, in ambient air and in dry air. The dry air had a relative humidity (RH) of <5% that was controlled by a sealed vial bottle containing silica gel.

An organic complementary inverter was fabricated on a flexible polyethylenenaphthalate (PEN) sheet. Compound **2** and 1,4-bis(4-methylstyryl)benzene (MeDSB) were used as *n*-type and *p*-type organic semiconductors, respectively. A 40 nm thick gold gate electrode was deposited on the surface of the PEN sheet followed by a 5 nm thick titanium adhesion layer. A 400 nm thick polymethylenemethacrylate (PMMA) was formed by spin-coating as the gate insulator providing a C_{ins} of 6 nF cm^{-2}. Organic semiconducting layers and gold source-drain electrodes were deposited by a method similar to that mentioned above for the OTFT fabricated on a silicon wafer. Inverter characteristics were measured with computer-controlled two-electrometer units (ADCMT8252) in dry air (RH < 5%).

2.4. Synthesis. *2.4.1. 2,5-Difluoro-1,4-terephthalonitrile (**3**).* To a suspension of cuprous cyanide (CuCN) (7.3 g, 82 mmol) and cuprous iodide (CuI) (4.0 g, 21 mmol) in nitrobenzene (55 mL) and DMF (165 L) was added 2,5-difluoro-1,4-dibromobenzene (2.7g, 10 mmol) dropwise at room temperature. Then, the mixture was refluxed for 20 h. After the mixture had cooled to room temperature, 2 N hydrochloric acid (HCl) (30 mL) and ferric chloride hexahydrate ($FeCl_3{\cdot}6H_2O$) (20 g) were added. The mixture was heated to 60 °C for 30 min. The resulting mixture was then cooled, extracted with dichloromethane, and washed five times with 6 N HCl, then with water, and then with brine, dried over anhydrous sodium sulfate, and filtered. The solvent was removed *in vacuo*, and then the residue was purified by column chromatography (19:1 hexane/ethyl acetate

Scheme 2. Synthetic Route to Compound 2

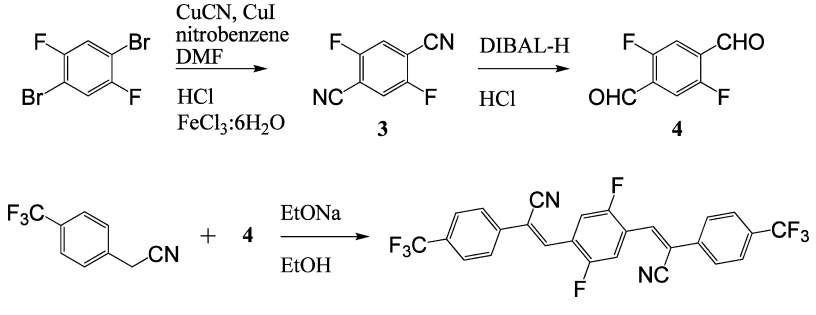

mixture) to give 2,5-difluoro-1,4-terephthalonitrile (0.73 g, 45% yield): ^{1}H NMR ($CDCl_3$) δ 7.55 (t, 2H, J = 7.2 Hz).

2.4.2. 2,5-Difluoro-1,4-terephthalaldehyde (4). To a solution of 2.5-difluoro-1,4-terephthalonitrile (**3**) (15.0 mg, 0.091 mmol) in toluene (15 mL) was added 1.02 M diisobutylaluminum hydride (DIBAL-H) (1.0 M in hexane, 0.23 mL, 0.23 mmol) at 0 °C. The reaction mixture was stirred for 1 h and then the reaction quenched with 2 N HCl (1.8 mL). The aqueous layer was extracted with ethyl acetate, washed with brine, dried over anhydrous sodium sulfate, and filtered. The solvent was removed *in vacuo*, and then the residue was purified by column chromatography (9:1 hexane/ethyl acetate mixture) to give 2,5-difluoro-1,4-terephthalaldehyde (**4**) (11.6 mg, 75% yield): ^{1}H NMR (400 MHz, $CDCl_3$) δ 10.38 (t, 2H, J = 1.2 Hz), 7.70 (t, 2H, J = 8.3 Hz), 7.83 (s, 2H), 7.76 (d, 4H, J = 8.3 Hz).

2.4.3. 2,5-Difluoro-1,4-phenylene-bis{2-[4-(trifluoromethyl)-phenyl]acrylonitrile} (2). To a solution of 4-(trifluoromethyl)-phenylacetonitrile (370.3 mg, 2.00 mmol) and 2,5-difluoro-1,4-terephthalaldehyde (**4**) (170.1 mg, 1.00 mmol) in ethanol (10 mL) was added a solution of sodium ethoxide (EtONa) (6.8 mg ,0.1 mmol) in ethanol (1.0 mL) dropwise at room temperature. The reaction mixture was stirred for 1 h by which time the product had precipitated. Precipitation was driven to completion by the dropwise addition of methanol. The precipitated yellow crystals were collected by filtration, washed with methanol, and dried in vacuum to yield 2,5-difluoro-1,4-phenylene-bis{2-[4-(trifluoromethyl)phenyl]acrylonitrile} (**2**) (469 mg, 93% yield). Further purification for fabrication of the OTFT was achieved by recrystallization from $CHCl_3$: mp 259–260 °C; ^{1}H NMR (400 MHz, $CDCl_3$) δ 8.21 (t, 2H, J = 8.4 Hz), 7.85 (d, 4H, J = 8.3 Hz), 7.83 (s, 2H), 7.76 (d, 4H, J = 8.3 Hz); ^{19}F NMR (470 MHz, $CDCl_3$) δ 66.1 (s, 6F), −120.2 (t, 2H, J = 8.5 Hz); ^{13}C NMR (125.6 MHz, THF-d_8) δ 157.8 (dd, J = 3.5, 250.9 Hz), 138.4, 134.2 (q, J = 2.3 Hz), 132.3 (q, J = 32.5 Hz), 127.9, 127.0 (q, J = 3.7 Hz), 126.3 (dd, J = 11.1, 13.1 Hz), 125.0 (q, J = 271.6 Hz), 117.1, 116.2 (dd, J = 9.5, 19.6 Hz), 116.0; MS (EI) m/z 504 (M^+). Anal. Calcd for $C_{26}H_{12}F_8N_2$: C, 61.91; H, 2.40; N, 5.55. Found: C, 61.80; H, 2.55; N, 5.64.

3. RESULTS AND DISCUSSION

3.1. Electrochemical Properties. The redox properties of compounds in solution were evaluated by CV calibrated using the ferrocene/ferrocenium (Fc/Fc^+) redox couple with a dichloromethane solution containing 0.1 M $TBAPF_6$ (Figure 1). The onset of reduction potential ($E_{red,onset}$) of compound **2**

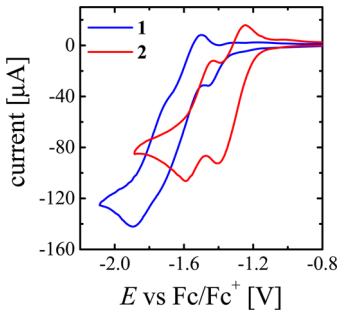

Figure 1. Cyclic voltammogram of compounds **1** (blue line) and **2** (red line) in solutions calibrated using the Fc/Fc^+ redox couple.

is 0.14 eV deeper than that of compound **1**. This indicates that the substituted fluorine atoms as further EWG moieties produced the deepening of the LUMO level of compound **2**. The LUMO levels of compounds were calculated using the equation $E^{LUMO} = -(E_{red,onset} + 4.8\ eV)$, in which 4.8 eV is the energy level of the Fc/Fc^+ couple below the vacuum level. The E^{LUMO} values of compounds **1** and **2** estimated from CV in solution were −3.56 and −3.70 eV, respectively. Besides the CV, the E^{LUMO} of a thin film of compound **1** estimated from E^{HOMO} by PYS and E_g was −4.1 eV. The energy levels of compounds **1** and **2** are summarized in Table S1 of the Supporting Information. These differences can be attributed to the difference in the state (solution or solid) as well as the difference in the measurement method (CV or PYS). The improved air stability of OTFT using compound **2** is expected from the relatively deeper LUMO level acting as a better chemical barrier than that of the OTFT using compound **1**.

3.2. Molecular Orientations. An AFM image of a deposited film of compound **2** (Figure 2) shows layer growth

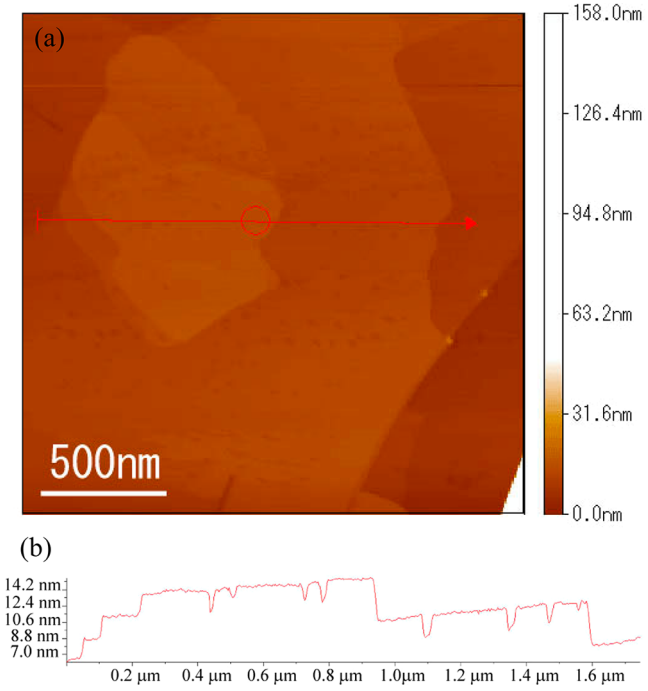

Figure 2. AFM image (a) and height profile (b) of the deposited film of compound **2**.

phenomena with ∼2 nm layer steps because the molecular length (2.04 nm by B3LYP/6-31G* calculations) is greater than and the surface profile is flatter than those of deposited compound **1**. The out-of-plane GIXD profile (q_z) of the deposited film of compound **2** presents typical periodicity with a d spacing value of ∼2 nm corresponding to a long molecular length (Figure 3). Besides this, the corresponding periodicities were not well displayed in the in-plane GIXD profile (q_{xy}). After substitution with fluorine atoms, a distinct difference in the molecular orientation in deposited compounds **1** and **2** was

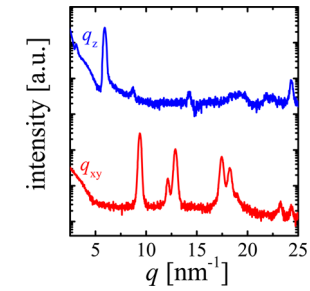

Figure 3. GIXD profiles of the deposited film of compound **2**. q_{xy} (red line) and q_z (blue line) curves display the in-plane and out-of-plane profiles, respectively.

dx.doi.org/10.1021/am404549e | ACS Appl. Mater. Interfaces 2014, 6, 3847−3852

not observed (Figures S1 and S2 of the Supporting Information). These findings indicate that the $\pi-\pi$ stacking direction is almost parallel to the substrate surface, which is suitable for in-plane charge carrier transport, and that the flat surface and the structured layer of fluorine atoms at molecular end-capped trifluoromethyl moieties can be provide an improved physical barrier for atmospheric oxidants penetrating into π-conjugated core units such as the passivation stacks.[8,9]

3.3. OTFT Characteristics. Figure 4 displays the (a) output and (b) transfer curves of the *n*-channel OTFT using compound **2** under vacuum operation, where I_D, V_D, and V_G represent the source-drain current, source-drain voltage, and source-gate voltage, respectively. I_D increases with a positive biasing of V_G, representing clear electron transport characteristics. The electron mobility (μ_e) of 0.170 cm^2 V^{-1} s^{-1} and the threshold voltage (V_T) of 5 V were estimated at a saturation regime at V_D of 100 V. The on/off current ratio exceeds 10^6, and the turn-on voltage (V_{ON}) is −10 V. Several measurements with individual OTFTs using compound **2** provide a highest μ_e of 0.389 cm^2 V^{-1} s^{-1} under vacuum operation. Despite several exposures to ambient air during device fabrication, the OTFTs persist with their relatively high performance of *n*-type transport characteristics. This indicates that our compound essentially possesses stable electron transport characteristics with respect to the atmospheric oxidants.

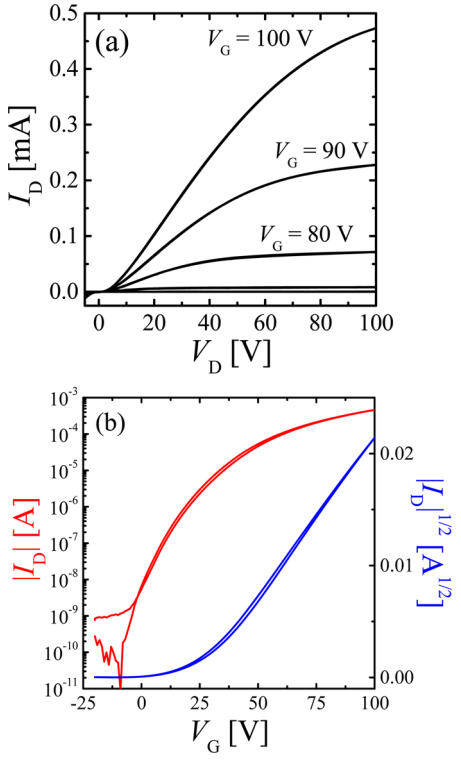

Figure 4. Output (a) and transfer (b) curve of OTFT using compound **2** under vacuum operation.

3.4. Air Stability. To confirm the air stability of the *n*-channel OTFT using compound **2**, the μ_e values in ambient air operation were investigated by comparing the transfer curves in the same device stored in a plastic box in ambient air and operated in ambient air and in the dark. The *n*-channel OTFT using compound **2** shows no μ_e degradation and a V_T shift (ΔV_T) after storage in ambient air for 1 day. The *n*-channel OTFT using compound **2** has robust air stability even with no passivation stacks. Figure 5 displays the time dependence in ambient air storage of the μ_e in ambient air operation of the *n*-channel OTFT using compound **2**. The OTFT using compound **2** has good long-term, air-stable *n*-channel OTFT properties in ambient air operation and shows a $\Delta\mu$ of only 40% and a ΔV_T of +22 V after storage in ambient air for 1 year. The $\Delta\mu$ values of air-stable *n*-type materials reported so far have been >50% after storage in ambient air for 6 months,[12−14,16−20] with the exception of the naphthalene-bis(dicarboximide)-based polymer.[15] This indicates that the electron transport characteristics in compound **2** are extremely robust against the atmospheric oxidants. Furthermore, the OTFT using compound **2** sealed in a vial bottle with silica gel showed a $\Delta\mu$ of only 3% and a ΔV_T of +5 V after storage in dry air with a relative humidity of <5% for 5 months (Figure 6 and Figure S3 of the Supporting Information). Therefore, a critical issue with respect to the degradation of *n*-channel OTFT properties was found to originate from the moisture in ambient air.[16,17] Compound **2** has sufficient long-term air stability under both ambient and dry conditions.

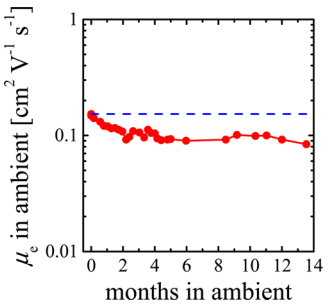

Figure 5. Ambient air exposure time dependence of the electron mobility in ambient air operation. The value of electron mobility under vacuum operation is indicated by a blue dashed line.

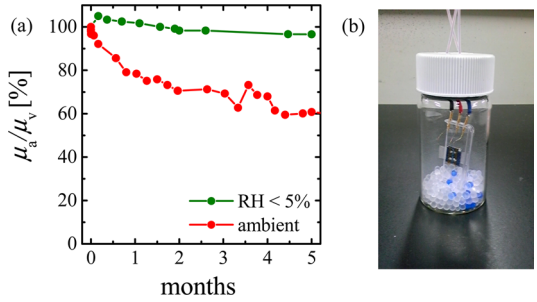

Figure 6. (a) Time dependence of the ratio of electron mobility in both ambient air and dry air. μ_v is the electron mobility under vacuum. μ_a is the electron mobility in air. The dry air condition with a RH of <5% was controlled by a sealed vial bottle containing silica gel as shown in panel b.

3.5. Complementary Inverter Characteristics. The organic complementary inverter was fabricated on a flexible PEN sheet with a PMMA insulator. Compound **2** and 1,4-bis(4-methylstyryl)benzene (MeDSB) were used as air-stable *n*-type and air-stable *p*-type organic semiconductors, respectively. MeDSB has a hole mobility of 0.13 cm^2 V^{-1} s^{-1}, which is similar to the carrier mobility value of compound **2**.[22] With the use of this combination of compound **2** and MeDSB for the organic complementary inverter, the balanced inverter performance is expected without reconstruction of device config-

urations, such as channel width and channel length. The characteristic of the organic complementary inverter after storage in dry air for 2 weeks, to prevent the degradation of PMMA, is shown in Figure 7, where V_{DD}, V_{IN}, and V_{OUT}

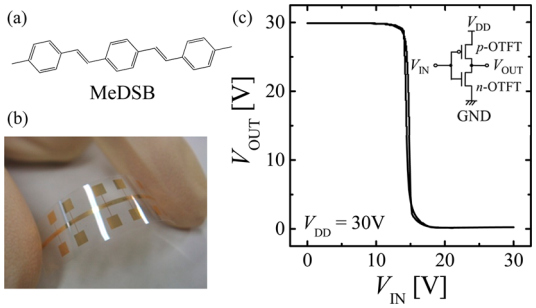

Figure 7. Characteristics of an organic complementary inverter fabricated on a plastic substrate (c), shown in a photograph (b), after storage in dry air (RH of <5%) for 2 weeks. MeDSB (a) and compound **2** were used as *p*-type and *n*-type semiconductors, respectively.

represent the drive voltage, the input voltage, and the output voltage, respectively. Figure 7 clearly displays the inverter switching curve that decreases with an increase in V_{IN}, and the balanced switching at a V_{IN} of 15 V, which is half of a V_{DD} of 30 V. The values of the signal gain dV_{OUT}/dV_{IN} are reaching −40 at a V_{IN} of 15 V (Figure S4 of the Supporting Information). The through current is very small, and the level of static power consumption is also small, several tens of nanowatts for a V_{DD} of 30 V. The input voltage difference at the half-output voltage of the full swing was designated as the amount of hysteresis (V_{hys}). There was no significant hysteresis behavior effect (V_{hys} of 0.4 V at a V_{OUT} of 15 V). This represents the fact that the device promises to operate with a reversal stable switching operation desired for a logic circuit. The obtained inverter performance is strong enough to apply the next stage logic circuit such as a ring oscillator, although the organic complementary inverter was operated in dry air after storage for 2 weeks.

4. CONCLUSION

We have successfully proven the existence of the extremely long-term air-stable *n*-channel OTFT with 2,5-difluoro-1,4-phenylene-bis{2-[4-(trifluoromethyl)phenyl]acrylonitrile}, compound **2**, which was synthesized by a high-yield simple procedure of Knoevenagel condensation. Bottom-gate top-contact-type OTFT devices using compound **2** showed typical *n*-channel OTFT characteristics with an electron mobility of >0.1 $cm^2 V^{-1} s^{-1}$. The fabricated OTFT also exhibited a high electron mobility of ∼0.1 $cm^2 V^{-1} s^{-1}$ in ambient air even after storage in ambient air for 1 year. The organic complementary inverter on a flexible PEN sheet using compound **2** and 1,4-bis(4-methylstyryl)benzene displayed good balanced inverter characteristics with a gain of −40 after storage in dry air for 2 weeks.

This long-term air stability of the *n*-channel OTFT using our compound was caused mainly by the physical barrier of the layer structured densely packed molecular end-capped trifluoromethyl moieties that probably formed the self-passivation stacks. Long-term air-stable *n*-type semiconducting compounds synthesized by a simple high-yield procedure might have great potential for further development and widespread use in organic electronics.

■ ASSOCIATED CONTENT

Supporting Information

Summary of energy levels of compounds **1** and **2**, AFM image of a deposited film of compound **1**, comparison of GIXD of compounds **1** and **2**, time dependence of ΔV_T of compound **2**, and signal gain characteristics of the organic inverter. This material is available free of charge via the Internet at http://pubs.acs.org.

■ AUTHOR INFORMATION

Corresponding Author

*E-mail: nagamatu@cse.kyutech.ac.jp.

Present Address

⊥S.O.: Graduate School of Science and Engineering, Yamagata University, Yamagata, Japan.

Notes

The authors declare no competing financial interest.

■ ACKNOWLEDGMENTS

This work was financially supported by the Kitakyushu Foundation for the Advancement of Industry Science and Technology (FAIS).

■ REFERENCES

(1) Katz, H. E.; Bao, Z.; Gilat, S. L. Synthetic Chemistry for Ultrapure, Processable, and High Mobility Organic Semiconductors. *Acc. Chem. Res.* **2001**, *34*, 359−369.

(2) Dimitrakopoulos, C. D.; Malenfant, P. R. L. Organic Thin Film Transistors for Large Area Electronics. *Adv. Mater.* **2002**, *14*, 99−117.

(3) Nagamatsu, S.; Kaneto, K.; Azumi, R.; Matsumoto, M.; Yoshida, Y.; Yase, K. Correlation of the Number of Thiophene Units with Structural Order and Carrier Mobility in Unsubstituted Even- and Odd-numbered α-Oligothiophene Films. *J. Phys. Chem. B* **2005**, *109*, 9374−9379.

(4) Dodabalapur, A.; Laquindanum, J.; Katz, H. E.; Bao, Z. Complementary Circuits with Organic Transistors. *Appl. Phys. Lett.* **1996**, *69*, 4227−4229.

(5) Haddon, R. C.; Perel, A. S.; Morris, R. C.; Palstra, T. T. M.; Hebard, A. F.; Fleming, R. M. C60 thin-film transistors. *Appl. Phys. Lett.* **1995**, *67*, 121−123.

(6) Laquindanum, J. G.; Katz, H. E.; Dodabalapur, A.; Lovinger, A. J. n-Channel Organic Transistor Materials Based on Naphthalene Frameworks. *J. Am. Chem. Soc.* **1996**, *118*, 11331−11332.

(7) Anthopoulos, T. D.; Anyfantis, G. C.; Papavassiliou, G. C.; de Leeuw, D. M. Air-stable ambipolar organic transistors. *Appl. Phys. Lett.* **2007**, *90*, 122105-1−122105-3.

(8) Jones, B. A.; Ahrens, M. J.; Yoon, M. H.; Facchetti, A.; Marks, T. J.; Wasielewski, M. R. High-Mobility Air-Stable n-Type Semiconductors with Processing Versatility: Dicyanoperylene-3,4:9,10-bis(dicarboximides). *Angew. Chem., Int. Ed.* **2004**, *43*, 6363−6366.

(9) Jones, B. A.; Facchetti, A.; Wasielewski, M. R.; Marks, T. J. High Mobility Air-Stable n-Type Perylene Diimide Semiconductors. Insight Into Materials Design for Stability of n-Type Charge Transport. *J. Am. Chem. Soc.* **2007**, *129*, 15259−15278.

(10) Chikamatsu, M.; Itakura, A.; Yoshida, Y.; Azumi, R.; Yase, K. High-Performance n-Type Organic Thin-Film Transistors Based on Solution-Processable Perfluoroalkyl-Substituted C_{60} Derivatives. *Chem. Mater.* **2008**, *20*, 7365−7367.

(11) Schmidt, R.; Oh, J. H.; Sun, Y. S.; Deppisch, M.; Krause, A.; Radacki, K.; Braunschweig, H.; Könemann, M.; Erk, P.; Bao, Z.; Würthner, F. High-Performance Air-Stable n-Channel Organic Thin Film Transistors Based on Halogenated Perylene Bisimide Semiconductors. *J. Am. Chem. Soc.* **2009**, *131*, 6215−6228.

(12) Shoji, K.; Nishida, J.; Kumaki, D.; Tokito, S.; Yamashita, Y. Synthesis and FET characteristics of phenylene-vinylene and anthracene-vinylene compounds containing cyano groups. *J. Mater. Chem.* **2010**, *20*, 6472−6478.
(13) Fujisaki, Y.; Nakajima, Y.; Kumaki, D.; Yamamoto, T.; Tokito, S.; Kono, T.; Nishida, J.; Yamashita, Y. Air-stable n-type organic thin-film transistor array and high gain complementary inverter on flexible substrate. *Appl. Phys. Lett.* **2010**, *97*, 133303-1−133303-3.
(14) Rödel, R.; Letzkus, F.; Zaki, T.; Burghartz, J. N.; Kraft, U.; Zschieschang, U.; Kern, K.; Klauk, H. Contact properties of high-mobility, air-stable, low-voltage organic n-channel thin-film transistors based on a naphthalene tetracarboxylic diimide. *Appl. Phys. Lett.* **2013**, *102*, 233303-1−233303-5.
(15) Yan, H.; Chen, Z.; Zheng, Y.; Newman, C.; Quinn, J. R.; Dötz, F.; Kastler, M.; Facchetti, A. A high-mobility electron-transporting polymer for printed transistors. *Nature* **2009**, *457*, 679−686.
(16) Ie, Y.; Nishida, K.; Karakawa, M.; Tada, H.; Asano, A.; Saeki, A.; Seki, S.; Aso, Y. Air-Stable n-Type Organic Field-Effect Transistors Based on Solution-Processable, Electronegative Oligomers Containing Dicyanomethylene-Substituted Cyclopenta[*b*]thiophene. *Chem.—Eur. J.* **2011**, *17*, 4750−4758.
(17) Ie, Y.; Ueta, M.; Nitani, M.; Tohnai, N.; Miyata, M.; Tada, H.; Aso, Y. Air-Stable n-Type Organic Field-Effect Transistors Based on 4,9-Dihydro-*s*-indaceno[1,2-*b*:5,6-*b*′]dithiazole-4,9-dione Unit. *Chem. Mater.* **2012**, *24*, 3285−3293.
(18) Yan, Z.; Sun, B.; Li, Y. Novel stable (3*E*,7*E*)-3,7-bis(2-oxoindolin-3-ylidene)benzo[1,2-*b*:4,5-*b*′]difuran-2,6(3*H*,7*H*)-dione based donor−acceptor polymersemiconductors for n-type organic thin film transistors. *Chem. Commun.* **2013**, *49*, 3790−3792.
(19) Lei, T.; Dou, J.; Cao, X.; Wang, J.; Pei, J. Electron-Deficient Poly(*p*-phenylene vinylene) Provides Electron Mobility over 1 cm^2 V^{-1} s^{-1} under Ambient Conditions. *J. Am. Chem. Soc.* **2013**, *135*, 12168−12171.
(20) Zhao, Y.; Guo, Y. L.; Liu, Y. Q. 25th Anniversary Article: Recent Advances in n-Type and Ambipolar Organic Field-Effect Transistors. *Adv. Mater.* **2013**, *25*, 5372−5391.
(21) Nagamatsu, S.; Moriguchi, T.; Nagase, T.; Oku, S.; Kuramoto, K.; Takashima, W.; Okauchi, T.; Mizoguchi, K.; Hayase, S.; Kaneto, K. A Steady Operation of n-Type Organic Thin-Film Transistors with Cyano-Substituted Distyrylbenzene Derivative. *Appl. Phys. Express* **2009**, *2*, 101502-1−101502-3.
(22) Yasuda, T.; Saito, M.; Nakamura, H.; Tsutsui, T. Control of *p*- and *n*-type carriers by end-group substitution in oligo-*p*-phenylenevinylene-based organic field-effect transistors. *Appl. Phys. Lett.* **2006**, *89*, 182108-1−182108-3.
(23) Greenham, N. C.; Moratti, S. C.; Bradley, D. D. C.; Friend, R. H.; Holmes, A. B. Efficient light-emitting diodes based on polymers with high electron affinities. *Nature* **1993**, *365*, 628−630.
(24) Chen, S. H.; Su, C. H.; Su, A. C.; Chen, S. A. Molecular Aggregation and Luminescence Behavior of Bulk Poly(2,5,2′,5′-tetrahexyloxy-8,7′-dicyano-di-*p*-phenylenevinylene). *J. Phys. Chem. B* **2004**, *108*, 8855−8861.